The Dam1 kinetochore complex harnesses microtubule dynamics to produce force and movement

Charles L. Asbury*[†], Daniel R. Gestaut[‡], Andrew F. Powers*, Andrew D. Franck*, and Trisha N. Davis[‡]

Departments of *Physiology and Biophysics and [‡]Biochemistry, University of Washington, Seattle, WA 98195

Kinetochores remain attached to microtubule (MT) tips during mitosis even as the tips assemble and disassemble under their grip, allowing filament dynamics to produce force and move chromosomes. The specific proteins that mediate tip attachment are uncertain, and the mechanism of MT-dependent force production is unknown. Recent work suggests that the Dam1 complex, an essential component of kinetochores in yeast, may contribute directly to kinetochore–MT attachment and force production, perhaps by forming a sliding ring encircling the MT. To test these hypotheses, we developed an *in vitro* motility assay where beads coated with pure recombinant Dam1 complex were bound to the tips of individual dynamic MTs. The Dam1-coated beads remained tip-bound and underwent assembly- and disassembly-driven movement over ≈3 μm, comparable to chromosome displacements *in vivo*. Dam1-based attachments to assembling tips were robust, supporting 0.5–3 pN of tension applied with a feedback-controlled optical trap as the MTs lengthened ≈1 μm. The attachments also harnessed energy from MT disassembly to generate movement against tension. Reversing the direction of force (i.e., switching to compressive force) caused the attachments to disengage the tip and slide over the filament, but sliding was blocked by areas where the MT was anchored to a coverslip, consistent with a coupling structure encircling the filament. Our findings demonstrate how the Dam1 complex may contribute directly to MT-driven chromosome movement.

cytoskeleton | DASH | disassembly | mitosis | motility

A long-standing mystery of mitosis is how kinetochores interact with the tips of microtubules (MTs) to organize and move chromosomes (1–3). A common view is that motor proteins of the kinesin and dynein families mediate tip attachment, but conventional motors cannot completely account for the interactions between kinetochores and MTs. Conventional motors bind and walk along the sides of the filaments (4, 5). In contrast, kinetochores remain attached to the filament tips even as the tips assemble and disassemble under their grip, undergoing back-and-forth movements that are tightly coupled to tip growth and shortening (2, 6). Even when conventional motors are removed or disrupted, kinetochores harness energy from MT disassembly to produce force and movement (2). Thus, kinetochores possess a nonconventional MT-based motility mechanism that relies on filament growth and shortening to drive movement.

Although a number of candidate MT-binding proteins are found at kinetochores, the relative contributions that these molecules make to MT-driven motility are unknown. In principle, "plus-end-tracking" proteins (+TIPs), which colocalize with growing MT tips in cells (7), might be involved. However, +TIPs are static with respect to the MT lattice (8, 9), and they have never been shown to mediate MT-driven cargo transport *in vitro*. Beads coated with inactivated kinesin and dynein motors can remain attached to disassembling MT tips *in vitro* (10), probably because the motors provide a large number of weak, transient binding interactions with the filaments (10, 11). But these motor-based tip attachments are sensitive to buffer conditions

(2, 10), and it is unclear whether they are robust enough to support the tensile loads supported by kinetochore–MT junctions *in vivo*. Furthermore, deletion of kinetochore motors in budding (12) and fission yeast (13, 14) causes relatively mild phenotypes, suggesting that kinetochore–MT attachment in these organisms may not require motors (3). Thus, considerable uncertainty remains about the molecular mechanism by which kinetochores maintain load-bearing attachments to MT tips.

Recent work suggests that the Dam1 complex (also called DASH or DDD), an essential component of kinetochores in yeast (15–17), makes a direct contribution to tip attachment and MT-driven movement. The Dam1 complex consists of 10 subunits that copurify as a stable heterodecamer (18, 19) with biochemical affinity for MTs (18, 20). The complex is required for sister kinetochores to make bipolar, load-bearing attachments to MTs from opposite spindle poles (21, 22). Electron microscopy reveals that when pure recombinant Dam1 is mixed with stabilized MTs, it oligomerizes into rings (each containing many individual complexes) that surround the filaments (19, 23). Theoretical considerations suggest that such rings may represent optimal structures for harnessing energy from MT disassembly to produce motion and force (24–26). Additional support for a direct role in MT attachment is provided by time-lapse fluorescence microscopy that shows Dam1 colocalizing with the tips of disassembling MTs *in vitro* (27). Although these observations are provocative, they do not establish whether the complex can link cargo to both assembling and disassembling tips or whether Dam1-based tip attachments support tension: two key properties that are necessary for persistent kinetochore-to-MT attachment *in vivo*. Moreover, evidence that the rings seen by electron microscopy are important for tip tracking or other Dam1 functions is lacking.

Using an *in vitro* motility assay, we show here that the Dam1 complex can couple cargo to the tips of individual dynamic MTs. Dam1-based tip attachments remain bound during both filament assembly and disassembly, moving several micrometers and supporting tension applied continuously with a feedback-controlled optical trap. These results demonstrate that the complex can contribute significantly to force production and MT-driven chromosome movement during yeast mitosis. We also find that Dam1-based linkages exhibit unique mechanical behaviors, such as sliding movements that are blocked by areas where the MT is anchored to a coverslip, which suggest a coupling structure encircling the MT.

Results

The Dam1 Complex Couples Cargo to Dynamic MT Tips. In our experiments, beads coated with the Dam1 complex were bound


BIOPHYSICS

PNAS
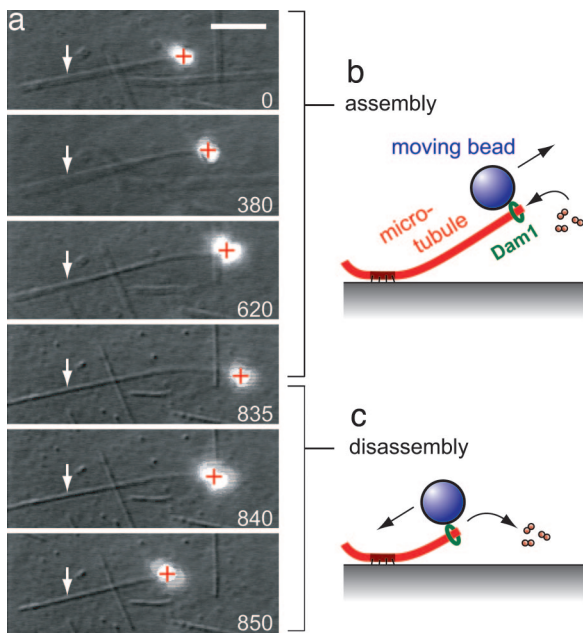
Fig. 1. Dam1 couples cargo to the tips of assembling and disassembling MTs. (*a*) Selected frames from a movie (Movie 1) in which movement of a Dam1-coated bead is driven by MT assembly (0–835 s) and disassembly (835–850 s). Approximate locations for the coverslip-anchored portion of the MT seed (arrows) and the bead center (plus signs) are indicated. Elapsed times are in seconds. (Scale bar, 5 μm.) (*b* and *c*) Schematic diagrams of the Dam1 bead motility assay. During assembly (*b*), the MT grows slowly by addition of tubulin subunits to the tip. During shortening (*c*), tubulin subunits are rapidly lost from the tip. During both phases, Dam1-based linkages remain tip-bound.

to the tips of individual dynamic MTs polymerized from stable, coverslip-anchored seeds (28, 29). The filaments exhibited dynamic instability typical for MTs *in vitro* (30), with periods of slow growth interrupted occasionally by rapid shortening that usually continued until the filament disassembled completely and just the seed remained. Dam1-coated beads were introduced into the slide and then tested for MT binding by using an optical trap (31–33). Each candidate bead was held near the tip of an assembling MT until it bound or until 1–2 min had passed without binding. Beads coated with the Dam1 complex frequently bound the MT tip (15%; 88 of 574 beads tested). Control beads without complex did not bind (89 beads tested). Dam1 beads that were active in MT binding could usually be reattached repeatedly to different MTs, and the fraction of active beads was not reduced when free complex was removed from the buffer by centrifugation (21%; 27 of 128 washed beads tested). These observations show that MT attachment depends on Dam1 complexes stably bound to the bead and suggest that free Dam1 in solution is not required.

The Dam1 complex mediated persistent attachment to the tip of a dynamic MT, allowing filament assembly and disassembly to drive bead movement (Fig. 1; see also Movies 1–3, which are published as supporting information on the PNAS web site). Initially, we recorded movement in the absence of external load by shutting off the optical trap after MT binding. During assembly without load, tip-attached beads moved away from the anchored MT seed as the length of intervening filament increased (Fig. 1*a*, 0–835 s, and Movie 1). Assembly-driven movement usually continued for several minutes, terminating in one of three ways: (*i*) the bead detached from the growing MT (≈41%); (*ii*) the bead remained attached but disengaged from the tip as the filament continued to lengthen (≈24%); (*iii*) the filament spontaneously underwent catastrophe, switching
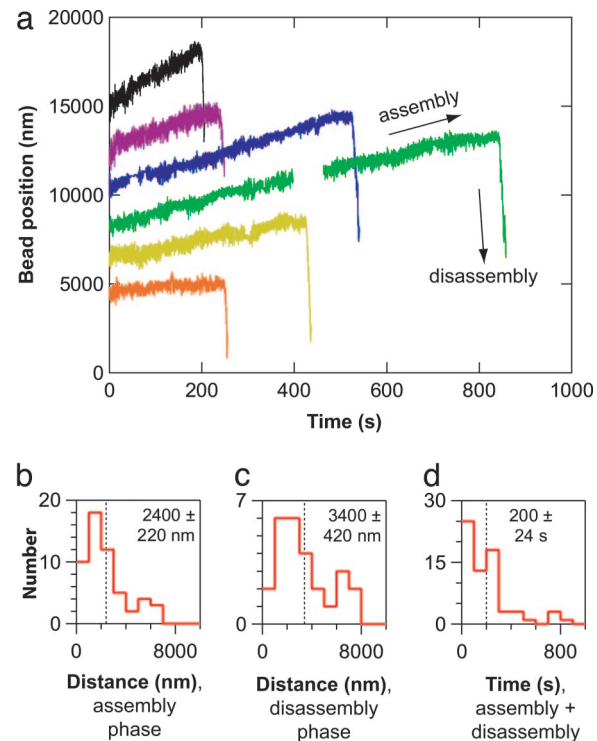
Fig. 2. MTs drive movement of Dam1-based linkages over several micrometers. (*a*) Records of bead position versus time measured without applied force showing slow assembly-driven movement followed by rapid disassembly-driven movement. Increasing position represents movement away from the anchored portion of the MT. For clarity, each record is offset vertically by an arbitrary amount. (*b*–*d*) Histograms of bead displacement during MT assembly (*b*), bead displacement during disassembly (*c*), and total duration (including both assembly and disassembly phases) of MT-driven movement (*d*) for a population of beads. Dotted vertical lines indicate the mean value for each histogram. These data were recorded at a tubulin concentration of 17 μM.

abruptly to rapid shortening (≈35%). After catastrophe, tip-attached beads were carried toward the seed in the direction of filament shortening (Fig. 1*a*, 835–850 s, and Movies 2 and 3). Disassembly-driven beads usually (≈96%) detached before the filament had shortened completely back to the seed (Movie 3 is an exception).

We quantified Dam1-based movement in the absence of load by tracking beads in video recordings (Fig. 2). On average, assembly-driven beads moved 2,400 ± 220 nm (average ± SEM, $n = 54$) before detaching, disengaging from the tip, or switching to disassembly-driven movement (Fig. 2*b*). Disassembly-driven beads moved 3,400 ± 420 nm ($n = 26$) before detaching (Fig. 2*c*). Periods of bead movement lasted 200 ± 24 s ($n = 67$; Fig. 2*d*), and the velocities of assembly- and disassembly-driven movement, 11 ± 1.0 nm·s^{-1} and 490 ± 46 nm·s^{-1}, respectively, were similar to growth and shortening rates for MTs alone (30). At the spatial resolution of these records (≈290 nm rms, limited by thermal motion of the bead), the movement usually appeared smooth (Fig. 2*a*).

The Dam1 Complex Supports Tension and Harnesses Energy from MTs to Produce Force. To apply tensile force in the bead assay, a tip-attached bead was held continuously in the optical trap, and its position was monitored by back focal plane interferometry (33) (Fig. 3). The force was kept constant by using a feedback-controlled piezoelectric stage to maintain a fixed offset between the bead and the trap center (31–33) (see Movies 4 and 5, which are published as supporting information on the PNAS web site).
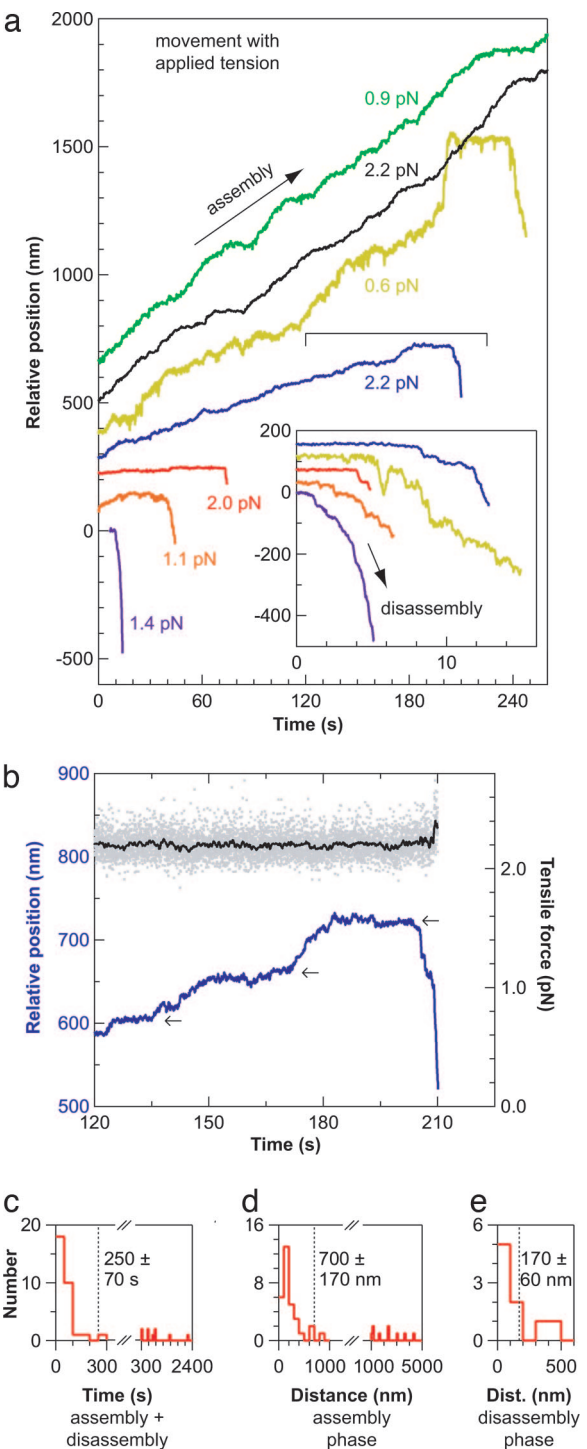
Fig. 3. Dam1-based linkages remain tip-attached even when tension is applied. (*a*) Records of bead position versus time during continuous application of tensile load by using a feedback-controlled optical trap. Increasing position represents assembly-coupled movement in the direction of applied force, away from the anchored portion of the MT (e.g., green and black traces and blue trace at <200 s). Some records terminate with episodes of disassembly-driven movement against the load (e.g., blue trace at 200–210 s), expanded views of which are shown in *Inset*. Records are offset vertically (and horizontally in *Inset*) for clarity. (*b*) Expanded view of the bracketed portion of the record in *a* showing transition from assembly- to disassembly-driven movement (blue trace). Arrows mark positions where the bead paused during movement. The measured bead-trap separation is shown in the upper plot (black trace; scale at right) after converting to force by multiplying by the trap stiffness. The gray dots show raw data, and the black trace shows the same data after smoothing with a 500-ms sliding boxcar

Even with 0.5–3 pN of continuous tension, the complex maintained a robust link to an assembling tip that persisted, on average, for 250 ± 70 s and moved 700 ± 170 nm in the direction of filament growth before detachment or catastrophe ($n = 40$; Fig. 3 *c* and *d*). Distributions of attached times and distances moved were broad and included very long events where attachment lasted >300 s and the bead moved >1,000 nm (Fig. 3 *c* and *d*). The applied tension reduced thermal fluctuations, allowing movement to be recorded with comparatively high spatial resolution (≈ 5 nm rms, depending on the series elastic compliance of the filament, the complex, etc). Viewed in finer detail, the movement appeared irregular, including pauses, rapid jumps, and periods of relatively smooth motion (Fig. 3 *a* and *b*).

The Dam1 complex harnessed energy released during MT disassembly to produce mechanical work. Linkages supporting tension during assembly-coupled movement sometimes remained attached long enough for the filament to undergo catastrophe (i.e. to switch from assembly to disassembly). When a catastrophe occurred, the bead usually reversed direction ($\approx 80\%$), moving against the applied force toward the MT seed (Fig. 3 *a Inset* and *b* and Movie 5). Moving against 0.5–3 pN of tension, beads traveled between 40 and 480 nm, with an average displacement of 170 ± 60 nm ($n = 9$; Fig. 3*e*). These observations show that Dam1-based tip attachments allow disassembling MTs to generate forces comparable to those produced by conventional motor proteins such as dynein and kinesin (32). We note that the 0.5–3 pN of tension we applied did not stall disassembly-driven movement, so higher forces can theoretically be produced. However, applied tension caused more frequent detachment of the bead from the MT, so episodes of disassembly-driven movement were observed less frequently, and they produced shorter displacements than in the absence of external load.

The Dam1 Complex Forms a Coupler That Slides Along the MT. We began each experiment by attaching a Dam1 bead to the tip of a filament. However, tip-attached beads undergoing assembly-driven movement without load sometimes disengaged from the tip but remained attached to the lattice (i.e., they stopped moving, and the tip grew beyond the point at which they were attached). Often, a brief pull toward the tip could reposition the bead onto the tip and restart assembly-driven movement. Conversely, pushing tip-attached beads toward the coverslip-anchored seed invariably caused them to disengage the tip and slide along the filament. By using feedback control to apply a pushing force of 0.2–1.3 pN, beads could be displaced by many micrometers along the MT without detachment ($n = 74$ sliding events averaging $5,100 \pm 300$ nm; Fig. 4*a*; see also Movies 6 and 7, which are published as supporting information on the PNAS web site). Several lines of evidence demonstrate that the beads remained attached during sliding. First, when the trap was shut off during sliding, the beads remained associated with the MT and underwent thermal motion synchronous with that of the filament ($n = 11$; Movies 8 and 9, which are published as supporting information on the PNAS web site). If detachment had occurred, the beads would simply have diffused away. Second, recorded position signals showed that frictional forces (0.2–1.3 pN) were transmitted to the beads during sliding. This friction was much greater than the viscous drag caused by movement through the surrounding fluid. Third, when beads reached the filament tips, sliding stopped ($n = 32$; Movies 6–9). If the beads had been free or had been bumping along the

average. (*c–e*) Histograms of total attached time (including both assembly and disassembly phases) (*c*), distance moved during assembly (*d*), and distance moved during disassembly (*e*) for tip-attached beads moving under 0.5–3 pN of tension. Dotted vertical lines indicate the means for each histogram. Tubulin concentration was 10 μM.
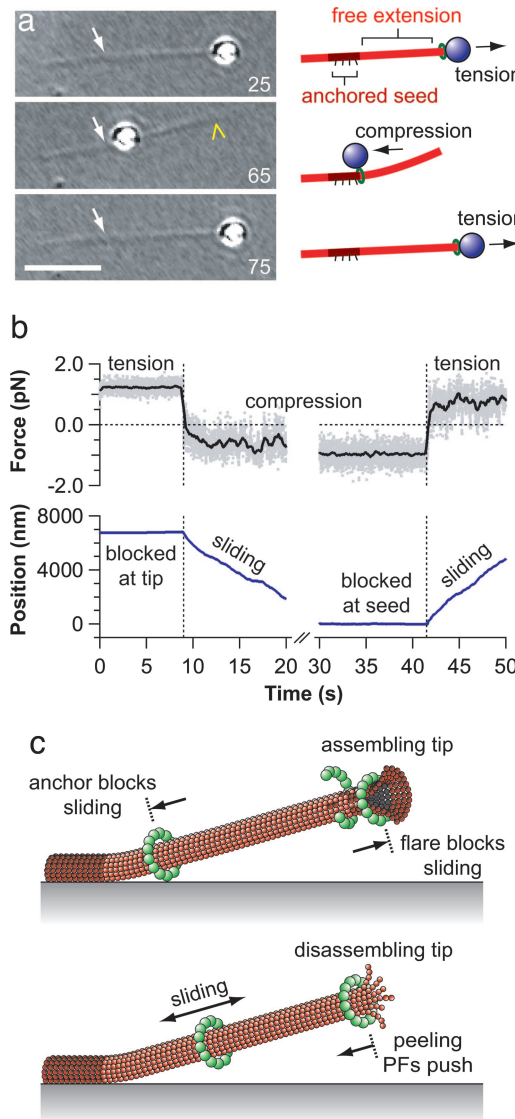
Fig. 4. Dam1-based couplers slide over the MT lattice without detaching, and both the growing tip and the coverslip-anchored portion of the MT present barriers to sliding. (*a*) Selected frames from a movie are shown (Movie 6), beginning with a tip-attached bead under tension (25 s). Reversing the direction of load (i.e., switching to compression) causes the bead to disengage the tip (denoted by the yellow chevron) and slide until it reaches the seed (white arrow), where sliding halts (65 s). Reversing the load again (i.e., reapplying tension) causes the bead to slide back and reengage the tip (75 s). (Scale bar, 5 μm.) (*b*) Beads located at the growing tip or the anchored seed respond asymmetrically to force: The same magnitude of force that is insufficient to slide them past the barrier, when reversed, immediately causes the bead to slide back away from the barrier. The lower plot shows bead position versus time, and the upper plot shows bead-trap separation after conversion to force by multiplying by the trap stiffness. Gray dots show raw data; black trace shows same data after smoothing with a 500-ms window. Dotted vertical lines mark the time when force was reversed. (*c*) Ring model for Dam1-based attachment and movement. In this view, between 10 and 16 Dam1 complexes (19, 27) oligomerize into a ring encircling the filament that is large enough to slide over the lattice (arrows) but too small to slide past areas where the filament is widened. Such a ring would be topologically prevented from sliding past the anchored segment of the MT (dotted line at left), as we observed. Growing tips also blocked sliding, perhaps because of the flared protofilament sheets that are thought to occur at assembling tips (38, 39). Protofilaments (PFs) curl and peel away from the main filament during disassembly (36, 37) and could push continuously against a Dam1 ring to drive movement in the direction of shortening. An alternative model in which coupling is provided by a disordered collection of MT-binding proteins is also consistent with our observations (see *Discussion*).

coverslip surface, the force clamp would have continued to push them past the tip of the filament.

Both the MT seed and the assembling tip presented barriers to sliding. When a sliding bead reached the anchored MT seed, movement halted (*n* = 23; Movies 6 and 7). If the direction of force was then reversed, the bead could be pulled back to the tip, where sliding stopped and the bead resumed assembly-coupled movement, which was slower and easily distinguished from sliding. The response to force at either barrier was asymmetric. The same magnitude of force that was insufficient to slide a bead past the anchored seed or the assembling tip, when reversed, could readily move it back from these barriers onto the intervening portion of the filament (*n* = 34 total observations, including 17 each at the tip and the seed; Fig. 4*b*). Importantly, there was no discernable delay between force reversal and the onset of sliding. This observation shows that the barrier-like behavior does not arise from a higher affinity of Dam1 for the seed or tip relative to the MT lattice.

In most of our experiments, the anchored MT seeds differed from the free extensions in their composition. The seeds contained guanylyl (α,β)methylenediphosphonate (GMPCPP) for stabilization, rather than GDP, and were biotinylated to facilitate anchoring to the coverslip (the ratio of biotinylated to native tubulin was 1:75). To test whether these differences were responsible for the barrier-like behavior at the seed, we grew uniform MTs with GMPCPP and biotin incorporated along their entire length. Dam1-coated beads bound readily and slid along these MTs. The barrier-like behavior was qualitatively unchanged (*n* = 26 total observations, including 13 each at the seed and the tip; Fig. 5, which is published as supporting information on the PNAS web site). This observation shows that blockage at the seed is not due to differences in MT composition.

Discussion

Our experiments demonstrate several remarkable and, to our knowledge, previously unobserved properties of the Dam1 complex, which indicate that it can contribute directly to MT attachment and MT-driven movement of kinetochores in yeast. We find that the complex can link cargo to both growing and shortening MT tips, allowing filament assembly and disassembly to drive movement over several micrometers (Figs. 1 and 2). Dam1-based linkages remain tip-bound for long times, even with applied tension (Fig. 3). The attached times, often >3 min, are similar to the time over which kinetochore–MT junctions support tension during mitosis in yeast, 2–10 min (21, 34). Yeast kinetochores in metaphase make MT-driven oscillatory movements 200–600 nm in amplitude (21, 35), and they are pulled ≈500 nm toward spindle poles in anaphase (35). We show here that Dam1 linkages allow MTs to drive movement *in vitro* over similar distances and to generate significant pulling forces in the 0.5- to 3-pN range. This level of force is similar to what is generated by ATP-powered motors that move various organelles inside living cells [e.g., neuronal vesicles, mitochondria, and pigment granules in melanophores (5)]. Thus, the Dam1 complex forms load-bearing tip attachments that are stable over the relevant time scale, that generate movement over relevant distances, and that produce forces sufficient to drive organelle movement. These observations, together with the established requirement for the Dam1 complex at kinetochores (15–17), strongly suggest that it makes a direct contribution to MT-driven kinetochore movement *in vivo*.

Thousands of tubulin subunits were added to or removed from the filament tip during a typical MT-driven movement in our assays, yet Dam1-based linkages remained tip-bound. This ability may depend on interactions with the GTP-containing subunits that cap growing tips or with unique structural features at the tips of growing and shortening MTs. During shortening, a disassembling tip becomes frayed as individual rows of subunits

(protofilaments) curl and peel away from the main filament before breaking off (36, 37). During growth, newly added subunits are thought to form a flared sheet that closes into a tube (38, 39).

An attractive model for Dam1-based MT attachment postulates that it depends on ring-like structures encircling the filament (19, 23, 25). In this view, an appropriately sized ring slides over the MT lattice but is unable to slide past areas where the filament is wider, such as a frayed tip. During disassembly, ring movement could be driven by biased diffusion (24, 25) or by a conformational wave where the frayed tip pushes continuously against the ring while propagating in the direction of shortening (25). Consistent with this picture, the Dam1 rings seen by electron microscopy appear large enough to slide over the filaments [32- to 35-nm ring inner diameter (19, 23) compared with ≈25-nm MT outer diameter (36)] but too small to slide past disassembling tips [typically ≈50 nm in width (36)]. However, electron microscopy studies of yeast kinetochores have so far failed to find evidence for rings *in vivo* (40). Observations of fluorescent-tagged Dam1 diffusing along stabilized MTs and accumulating at disassembling MT tips during filament shortening (23, 27) are also consistent with the ring model, but these activities can be explained by alternative mechanisms that do not depend on rings. One such mechanism, for example, has been proposed where coupling is provided by a disordered collection of proteins with weak MT affinity to explain the disassembly-driven movement of motor-coated beads (10). Thus, an important open question is whether the rings that Dam1 forms around MTs are functionally significant.

We found by direct manipulation that Dam1-based attachments slide along the MT when they are pushed with an optical trap and that both growing tips and coverslip-anchored seeds present barriers to sliding (Fig. 4*a*). Once a Dam1 coupler comes in contact with either barrier, it responds asymmetrically to force: If the direction of force is maintained (i.e., the force is directed toward the barrier), no further movement occurs, but if the direction of force is reversed, the coupler slides immediately back away from the barrier (Fig. 4*b*). These behaviors are predicted for a ring or collar that closely surrounds the filament. Such a collar would be topologically prevented from sliding past the coverslip-anchored seed but would slide back immediately upon force reversal, because the blockage occurs for purely structural reasons. A similar structural picture can explain the barrier-like behavior at assembling tips. Flared protofilament sheets are thought to occur at growing MT tips (38, 39). If the flares are wide enough, they will also block ring sliding (Fig. 4*c*). An alternative interpretation is also possible in which coupling is based on biochemical or electrostatic affinity for the MT. Weak affinity for the MT lattice could produce a coupler that slides along the filament without detaching (10, 11, 24), and an abrupt loss of affinity at the seed or the tip might present an energetic barrier that prevents sliding past these locations (24). However, blockage at the seed does not arise from differences in biotin labeling or guanylyl (α,β)methylenediphosphonate incorporation (Fig. 5), arguably the two features most likely to alter affinity of Dam1 for the seed. Based on these considerations, we think that coupling in our assays is more likely to depend on Dam1-based structures that encircle the filaments. We note that our beads are coated with many Dam1 complexes (presumably thousands), so their attachment to MTs probably involves many individual complexes. The minimum number of complexes and the structural requirements for attachment have yet to be determined.

In summary, we have demonstrated how the Dam1 complex can contribute directly to kinetochore–MT attachment and chromosome movement in yeast by forming load-bearing attachments to both growing and shortening MT tips. By direct manipulation, we show that Dam1-based MT attachments ex-

hibit unique mechanical properties that are consistent with a coupling structure encircling the filament. Our biophysical approach may be useful for further testing this hypothesis and for studying various functional aspects of Dam1 and other MT-binding kinetochore components.

Materials and Methods

Protein Purification. All ten subunits of the Dam1 complex were expressed in *Escherichia coli* (BL21 Rosetta, Novagen) from a single plasmid (a gift from J. J. Miranda, Harvard University, Boston) and purified essentially as described in refs. 19 and 23. The gene for one subunit (Spc34p) included a His-6 tag to facilitate purification and bead binding. Cells harboring the plasmid were induced to express the complex in midlogarithmic phase by addition of 0.2 mM IPTG, grown for 5 h at 37°C, pelleted, and snap-frozen. Pellets were resuspended in PB [20 mM phosphate, pH 7.0/500 mM NaCl/1 mM PMSF/complete protease inhibitors without EDTA (Roche Diagnostics)], lysed in a French press, and clarified by centrifugation. The supernatant was mixed with metal-affinity resin (Talon, BD Biosciences), washed in PB, and eluted with 200 mM imidazole. The eluate was purified on a size-exclusion column (Superdex 200 10/300GL, Amersham Pharmacia Biosciences), equilibrated with PB, and snap-frozen in 5-μl aliquots.

Motility Assays. To bind the His-6-tagged complex, 0.44-μm-diameter streptavidin-coated polystyrene beads (Spherotech, Libertyville, IL) were further functionalized by incubation with biotinylated penta-His antibody (Qiagen, Valencia, CA) and washed in BRB80 (80 mM Pipes/1 mM MgCl$_2$/1 mM EGTA, pH 6.9) plus 8 mg·ml^{-1} BSA, which was included as a blocking protein. Beads functionalized with anti-His antibody were used for the negative binding control experiments. Dilute suspensions of anti-His beads (0.01–0.05% solids) were coated with Dam1 by mixing with a 0.2–6.5 μM concentration of the complex in BRB80 plus BSA and incubating >30 min. In many experiments, free Dam1 was removed from the beads by centrifugation before introducing them into the flow chamber. Washing away free complex did not significantly change the behavior of MT-attached beads, so data from washed and unwashed beads are combined in Fig. 2. The experiments with applied force (i.e., Figs. 3–5) were performed with washed beads. Stable MT seeds were grown by incubating 68 μM bovine brain tubulin, 1 μM biotinylated tubulin (Cytoskeleton, Denver), and 1 mM guanylyl (α,β)methylenediphosphonate (Jena Bioscience, Jena, Germany) in BRB80 plus 10% glycerol at 37°C for >30 min. KOH-cleaned coverslips were fixed with double-stick tape to glass slides to create flow chambers, which were functionalized by incubation with 5 mg·ml^{-1} biotinylated BSA (Vector Laboratories) followed by 1 mg·ml^{-1} avidin DN (Vector Laboratories). Seeds were bound and then washed with GB (BRB80 plus BSA with 1 mM GTP) before introduction of Dam1 beads and tubulin (at indicated concentrations) in GB supplemented with 1 mM DTT and an oxygen scavenging system consisting of 250 μg·ml^{-1} glucose oxidase/30 μg·ml^{-1} catalase/4.5 mg·ml^{-1} glucose. After MT growth, thermal fluctuations tended to bend the extensions slightly away from the coverslip, making them easily distinguishable from coverslip-bound seeds and making their tips accessible for bead binding. All values reported in the text are mean ± SEM unless otherwise noted. Assays were performed at 22°C.

Instrumentation and Data Collection. The optical trap was essentially as described in refs. 31–33, except that a single laser was used for trapping and position detection and it was not steered by acoustooptic deflectors. For assays without applied load, bead positions were tracked in recorded videos at 30 Hz by using custom software written in LABVIEW (National Instruments,

Austin, TX). For the force-clamp assays, position sensor response was mapped by using the piezo stage to raster-scan a stuck bead through the beam, and trap stiffness was calibrated along the two principal axes by using the drag force, equipartition, and power spectrum methods (33). Feedback was implemented with custom LABVIEW software. During clamping, bead-trap separation was sampled at 40 kHz while stage position was updated at 50 Hz to maintain the desired load. Bead and stage position data were decimated to 200 Hz before storing to a disk. To minimize force errors, trap stiffness was chosen so that bead-trap separations >50 nm achieved the desired load (33). To slide Dam1 beads along MTs over distances >500 nm, it was helpful to apply load gently by using feedback control to keep the force <1 or 2 pN. Manually applying load with hand micrometers or a joystick-operated piezo usually caused detachment.

1. Gadde, S. & Heald, R. (2004) *Curr. Biol.* **14,** R797–R805.
2. Inoue, S. & Salmon, E. D. (1995) *Mol. Biol. Cell* **6,** 1619–1640.
3. McIntosh, J. R., Grishchuk, E. L. & West, R. R. (2002) *Annu. Rev. Cell Dev. Biol.* **18,** 193–219.
4. Howard, J. (1996) *Annu. Rev. Physiol.* **58,** 703–729.
5. Vale, R. D. (2003) *Cell* **112,** 467–480.
6. Skibbens, R. V., Skeen, V. P. & Salmon, E. D. (1993) *J. Cell Biol.* **122,** 859–875.
7. Schuyler, S. C. & Pellman, D. (2001) *Cell* **105,** 421–424.
8. Perez, F., Diamantopoulos, G. S., Stalder, R. & Kreis, T. E. (1999) *Cell* **96,** 517–527.
9. Tirnauer, J. S., Grego, S., Salmon, E. D. & Mitchison, T. J. (2002) *Mol. Biol. Cell* **13,** 3614–3626.
10. Lombillo, V. A., Stewart, R. J. & McIntosh, J. R. (1995) *Nature* **373,** 161–164.
11. Peskin, C. S. & Oster, G. F. (1995) *Biophys. J.* **69,** 2268–2276.
12. Cottingham, F. R., Gheber, L., Miller, D. L. & Hoyt, M. A. (1999) *J. Cell Biol.* **147,** 335–350.
13. Garcia, M. A., Koonrugsa, N. & Toda, T. (2002) *Curr. Biol.* **12,** 610–621.
14. West, R. R., Malmstrom, T., Troxell, C. L. & McIntosh, J. R. (2001) *Mol. Biol. Cell* **12,** 3919–3932.
15. Cheeseman, I. M., Enquist-Newman, M., Muller-Reichert, T., Drubin, D. G. & Barnes, G. (2001) *J. Cell Biol.* **152,** 197–212.
16. Jones, M. H., He, X., Giddings, T. H. & Winey, M. (2001) *Proc. Natl. Acad. Sci. USA* **98,** 13675–13680.
17. Li, Y., Bachant, J., Alcasabas, A. A., Wang, Y., Qin, J. & Elledge, S. J. (2002) *Genes Dev.* **16,** 183–197.
18. Cheeseman, I. M., Brew, C., Wolyniak, M., Desai, A., Anderson, S., Muster, N., Yates, J. R., Huffaker, T. C., Drubin, D. G. & Barnes, G. (2001) *J. Cell Biol.* **155,** 1137–1145.
19. Miranda, J. J., De Wulf, P., Sorger, P. K. & Harrison, S. C. (2005) *Nat. Struct. Mol. Biol.* **12,** 138–143.
20. Hofmann, C., Cheeseman, I. M., Goode, B. L., McDonald, K. L., Barnes, G. & Drubin, D. G. (1998) *J. Cell Biol.* **143,** 1029–1040.
21. He, X., Rines, D. R., Espelin, C. W. & Sorger, P. K. (2001) *Cell* **106,** 195–206.
22. Janke, C., Ortiz, J., Tanaka, T. U., Lechner, J. & Schiebel, E. (2002) *EMBO J.* **21,** 181–193.
23. Westermann, S., Avila-Sakar, A., Wang, H. W., Niederstrasser, H., Wong, J., Drubin, D. G., Nogales, E. & Barnes, G. (2005) *Mol. Cell* **17,** 277–290.
24. Hill, T. L. (1985) *Proc. Natl. Acad. Sci. USA* **82,** 4404–4408.
25. Koshland, D. E., Mitchison, T. J. & Kirschner, M. W. (1988) *Nature* **331,** 499–504.
26. Molodtsov, M. I., Grishchuk, E. L., Efremov, A. K., McIntosh, J. R. & Ataullakhanov, F. I. (2005) *Proc. Natl. Acad. Sci. USA* **102,** 4353–4358.
27. Westermann, S., Wang, H. W., Avila-Sakar, A., Drubin, D. G., Nogales, E. & Barnes, G. (2006) *Nature* **440,** 565–569.
28. Dogterom, M. & Yurke, B. (1997) *Science* **278,** 856–860.
29. Janson, M. E., de Dood, M. E. & Dogterom, M. (2003) *J. Cell Biol.* **161,** 1029–1034.
30. Walker, R. A., O'Brien, E. T., Pryer, N. K., Soboeiro, M. F., Voter, W. A., Erickson, H. P. & Salmon, E. D. (1988) *J. Cell Biol.* **107,** 1437–1448.
31. Asbury, C. L., Fehr, A. N. & Block, S. M. (2003) *Science* **302,** 2130–2134.
32. Block, S. M., Asbury, C. L., Shaevitz, J. W. & Lang, M. J. (2003) *Proc. Natl. Acad. Sci. USA* **100,** 2351–2356.
33. Lang, M. J., Asbury, C. L., Shaevitz, J. W. & Block, S. M. (2002) *Biophys. J.* **83,** 491–501.
34. Sanchez-Perez, I., Renwick, S. J., Crawley, K., Karig, I., Buck, V., Meadows, J. C., Franco-Sanchez, A., Fleig, U., Toda, T. & Millar, J. B. (2005) *EMBO J.* **24,** 2931–2943.
35. Pearson, C. G., Maddox, P. S., Salmon, E. D. & Bloom, K. (2001) *J. Cell Biol.* **152,** 1255–1266.
36. Mandelkow, E. M., Mandelkow, E. & Milligan, R. A. (1991) *J. Cell Biol.* **114,** 977–991.
37. Tran, P. T., Joshi, P. & Salmon, E. D. (1997) *J. Struct. Biol.* **118,** 107–118.
38. Chretien, D., Fuller, S. D. & Karsenti, E. (1995) *J. Cell Biol.* **129,** 1311–1328.
39. Wang, H. W. & Nogales, E. (2005) *Nature* **435,** 911–915.
40. McIntosh, J. R. (2005) *Nat. Struct. Mol. Biol.* **12,** 210–212.